Journal of Molecular Catalysis B: Enzymatic 60 (2009) 163–170

Contents lists available at ScienceDirect

Journal of Molecular Catalysis B: Enzymatic

journal homepage: www.elsevier.com/locate/molcatb

Biocatalytic capture of CO_2 with carbonic anhydrase and its transformation to solid carbonate

Nathalie Favre, M. Lorraine Christ, Alain C. Pierre*

Université Lyon 1, CNRS, UMR 5256, IRCELYON, Institut de recherches sur la catalyse et l'environnement de Lyon, 2 Avenue Albert Einstein, F-69626 Villeurbanne, France

ARTICLE INFO

Article history:
Received 30 October 2008
Received in revised form 29 April 2009
Accepted 29 April 2009
Available online 6 May 2009

Keywords:
Carbon dioxide
Calcium carbonate
Formation kinetics
Biocatalysis
Carbonic anhydrase

ABSTRACT

Atmospheric CO_2 is well known to be a major contributor to the "green house" effect on earth and as such it deserves to be treated as any environmental pollutant. The present paper focused on its biocatalytic capture by an anhydrase carbonic enzyme to form HCO_3^- anions, followed by trapping as solid $CaCO_3$ in basic conditions, in a "one pot" process. The kinetics of $CaCO_3$ formation with and without enzyme were compared at 5 and 20 °C, as well as the crystalline nature of the solid formed. Depending on the temperature and the initial pH of the buffer used, two different solid phases were observed: metastable vaterite and stable rhombohedra calcite. The formation of vaterite was enhanced when a buffer stock solution at an initial pH of 10.5, without any enzyme, was used. The possible mechanisms to explain these observations are discussed. At 5 °C, the initial precipitation rate of solid $CaCO_3$ increased by the addition of the enzyme, by a multiplication factor >10. However, this initial rate was also found to depend on the concentration of enzyme and the buffer capacity. Depending on these two parameters, an increasing formation rate of HCO_3^- in a first step, may lower the reaction medium pH so quickly, that the precipitation of solid carbonate in a second step may be highly hindered. As a consequence, the overall formation rate of solid $CaCO_3$ may actually decrease, for instance when the mass of enzyme is increased.

1. Introduction

The capture and sequestration of atmospheric CO_2 is considered as a problem of general interest which requires large scale solutions. Many articles have addressed this subject and reviews of the possible techniques which can be applied have been published, for instance by Benson and Surles [1]. The task comprises, first capturing the CO_2, secondly storing or transforming it. Capture can be done for instance by membrane separation, including liquid membranes containing amines [2] or carbonic anhydrase enzymes [3], adsorption on solids [4] or direct reaction with compounds such as minerals [5]. The most frequently investigated storing technique of CO_2 is as a gas under high pressure in geological formations, such as exhausted mines [1]. CO_2 can also be used as a substrate to synthesize valuable chemicals, as reviewed by Sakakura et al. [6] or it may simply be transformed and stored as solid carbonates [7].

In the present work we focused on the use of a carbonic anhydrase enzyme (further termed CA) in aqueous solution. This type of enzyme is known to catalyze the reactions involved in the equilibrium between the $CO_{2(aq)}$ molecules in solution on one hand and the HCO_3^- anions on the other hand. In particular some varieties of this enzyme exert important actions in the human body, in neutral conditions [8]. Besides, this enzyme is extremely selective. As an example, it can be used to efficiently separate $CO_{2(g)}$ from other gases such as N_2, O_2 and atmospheric pollutants when dissolved in liquid membranes, as developed by NASA [3]. According to their work, CA containing liquid membranes were found to be significantly faster than similar membranes containing amines instead of CA, to the point that the rate limiting step was the diffusion of HCO_3^- anions from one side to the other side of the membrane [9].

At last CA can be used to precipitate a solid, such as $NaHCO_3$ in appropriate pH conditions and when an appropriate source of Na salt is added, in particular concentrated industrial or ocean derived brines [7]. Bond et al. [10,11] used various industrial brines containing Ca^{2+} cations as well as Mg^{2+} cations. They measured the onset time of $CaCO_3$ precipitate formation, the fall rate of the pH [12], the [Ca] concentration by flame atomic absorption before and after precipitation and the [CO_2] concentration in solution as the "total inorganic carbon" in a "TOC" carbon analyzer. In a second setup, the enzyme was immobilized in chitosan–alginate beads to catalyze the formation of HCO_3^- anions in a pH range from 8.55 to 8.7 and the Ca^{2+} containing brine was added in a further step. In another study, Mirjafari et al. studied the precipitation of $CaCO_3$ from a model brine made by aqueous dissolution of $CaCl_2{\cdot}2H_2O$ in a buffer solution containing the CA enzyme. They measured the mass of $CaCO_3$ precipitated as a function of time, after addition of a $CO_{2(g)}$ saturated solution [13]. They also followed the onset of

* Corresponding author. Tel.: +33 4 72 44 53 38.
E-mail address: Alain.Pierre@ircelyon.univ-lyon1.fr (A.C. Pierre).

1381-1177/$ – see front matter © 2009 Elsevier B.V. All rights reserved.
doi:10.1016/j.molcatb.2009.04.018

precipitation by measuring the solution turbidity as a function of time.

For industrial applications, industrial brines should be used as calcium sources, as Bond et al. did [10,11]. Calcium chloride is itself industrially produced from calcium carbonate and cannot be used as a good industrial substrate. However, this salt makes it possible to design model brines with a simple and well defined composition, in a first step. Hence, in the present study, the kinetics of $CaCO_3$ precipitation from $CaCl_2$ in basic conditions were studied. Precipitation of this solid was examined at two temperatures, with the free CA enzyme as well as without enzyme as done in the work of Mirjafari et al. [13]. Moreover, the influence of the initial $[CO_{2(aq)}]$ aqueous concentration, buffer ionic strength and capacity and mass of enzyme, were studied. The crystallographic nature and crystal shape of the solid formed were also determined by X-ray diffraction and scanning electron microscopy.

2. Materials and methods

2.1. Materials

The carbonic anhydrase (CA) enzyme from bovine erythrocytes (E.C. 4.2.1.1) used in the present study was purchased as a white lyophilized salt free powder from SERVA Electrophoresis (Germany). The specific commercial concentration of this preparation was ≈1.3 U/mg, where 1 U is the amount of enzyme which catalyzes the hydrolysis of 1 μmol p-nitrophenylacetate per minute at 25 °C and pH 7.6. In most reactions presently catalyzed with this enzyme, a total CA content of 5.2 U and concentration ≈0.193 U mL^{-1} was used. However, in one series of tests, the influence of the total quantity of CA enzyme, in a range from 0 to 10.4 U, was studied.

The CO_2 used (standard grade) was purchased from the "Air Liquide" company as 50 L bottles under a pressure of ≈50 MPa. It was bubbled in water at a pressure of ∼0.1 MPa during 60 min. The water used to perform the carbonation reaction was HPLC grade ultra-pure, prepared with an ELGA PURELAB UHQ water purification system. $CaCl_2{\cdot}2H_2O$ (99.5%) was purchased from Aldrich. Its initial concentration in the final mixture was ≈0.076 M and its initial contribution to the mixture ionic strength ≈0.082. These initial values were identical in all experiments.

Tris–HCl buffer (pH 10.5; 9.4 and 8.4) were prepared by mixing 12.5 mL of Tris hydroxymethyl)aminomethane (Tris: Fluka 1.4 M) with increasing volumes of HCl (Prolabo, 1.4 M) and completing to 25 mL with deionized water. This buffer was provided as a soluble solid powder, which gives a pH ≈10.5 when dissolved in water at a concentration of 1.4 M. The buffering equilibrium reaction of Tris can be written as:

$$RNH_2 + H^+ \rightleftarrows RNH_3{}^+ \qquad pK_a \approx 8.1 \tag{1}$$

where R designates $(HOCH_2)_3C$.

While the CA enzyme is known to operate at pH ≈7 in human bodies [8], solid $CaCO_3$ forms at higher pH. Hence, a compromise was a priori selected in the present study, as this "Tris" buffer has an intermediate pK_a (≈8.1). This buffer is also often used with other enzymes. The buffer capacity β and ionic strength I, first in each buffer stock solution before use, secondly in the reaction medium after 1 min reaction, are gathered in Table 1. The buffer capacity considered here is defined as the derivative $d\,n(RNH_3{}^+)/d(pH)$ where $d\,n(RNH_3{}^+)$ is the incremental mole number of Tris transformed for a pH increment d(pH). As this table shows, both the ionic strength I and the capacity β increased in the buffer stock solutions, as the pH decreased from 10.5 to 8.4, because the buffer was gradually brought closer to its pK_a.

2.2. Solids characterization

The solids precipitated were analyzed by X-ray diffraction with the Cu Kα radiation (λ = 0.154 nm) on a Bruker D5005 Theta–theta vertical diffractometer equipped with a graphite monochromator. On selected samples, scanning electron microscopy was performed on a JEOL JSM 5800 LV electron microscope under an electrical tension of 20 kV. For this purpose, a small solid piece of each sample to be examined was placed on a sample holder covered with a carbon tab and metallized with gold during 2.5 min in a cathodic atomizer blazer. Some Fourier transformed infrared (FTIR) transmission spectra were also recorded on a Bruker IFS-48 Vector 22 FTIR spectrometer. The samples were prepared as KBr compressed pellets containing ≈1% (by mass) of the precipitate powder (≈2 mg precipitate powder and ≈300 mg of KBr powder).

2.3. Assay of the catalytic activity and parameters studied

In a first step, a volume X (from 1 to 20 mL) of pure HPLC water was placed in a 2-necked 100 mL spherical flask. Some $CO_{2(g)}$ gas was bubbled in the water, through a needle dipping in this water. The $CO_{2(g)}$ was flowed under a pressure of ≈0.1 MPa, during 60 min, from a CO_2 bottle. During this operation, the solution was maintained under constant agitation at a speed of 800 rpm with a magnetic stirrer and the flask was open to the ambient air. When $CO_{2(g)}$ bubbling was stopped, both flask openings were immediately closed with a rubber cap. Hence, the initial atmosphere above the water was essentially $CO_{2(g)}$ gas at an initial pressure $p(CO_{2(g)})_0 \approx 0.1$ MPa.

In a second step, a volume T (from 1 to 10 mL) of Tris–HCl buffer, at a specific pH of 8.4, 9.4 or 10.5, was added into the flask water with a syringe, through the rubber cap to maintain the $CO_{2(g)}$ pressure at 0.1 MPa. Two tests were always carried out in parallel, one in which a total quantity of 5.2 U of CA enzyme ($m_{enz} \approx 4$) was previously dissolved in the buffer, another one without any enzyme. In some experiments, the reaction flask was cooled with an ice bath (temperature inside the glass reactor maintaining at ≈5 °C).

Table 1
pH, buffer ionic strength and buffer capacity defined by the derivative $d\,n(RNH_3{}^+)/d(pH)$, in the buffer stock solutions and in the reaction medium after 1 min reaction, at 20 °C.

	Buffer stock solutions			Reaction medium after 1 min		
	pH_s	I_s	β_s	pH_1	I_1[a]	β_1
Without enz.	10.5	7.80×10^{-6}	0.0071	8.32	8.15×10^{-5}	0.070
With enz.				8.02	1.72×10^{-4}	0.074
Without enz.	9.4	1.12×10^{-3}	0.0733	7.66	3.10×10^{-4}	0.058
With enz.				7.19	4.57×10^{-4}	0.029
Without enz.	8.4	5.46×10^{-2}	0.359	6.99	4.96×10^{-4}	0.020
With enz.				6.92	5.07×10^{-4}	0.017
Initial $CaCl_2$ contribution					0.082	

[a] Contribution of the buffer to the reaction medium ionic strength.

Immediately after, in a third step, a volume Y of HPLC water in which 0.3 g of $CaCl_2{\cdot}2H_2O$ (2.054 mmol) was previously dissolved, was also introduced with a syringe in the flask through the rubber septum. The stirring speed was then increased to 1200 rpm and maintained for a given reaction time t (from 1 to 15 min). After this time, the flask content was filtered and the dry mass of solid precipitated was determined. The liquid medium pH was also immediately measured with an Ag/AgCl saturated electrode coupled with a pH meter (Analytical PHC 3001-9).

In all tests, the total aqueous volume ($X+T+Y$) was ≈27 mL. The initial concentration of $CaCl_2{\cdot}2H_2O$ was 76 mM and the initial $CaCl_2$ contribution to the reaction medium ionic strength was 0.082. Moreover, a volume of ≈73 mL $CO_{2(g)}$ at initial pressure ~0.1 MPa corresponding to 3.12 mmol $CO_{2(g)}$ introduced during the initial bubbling step, was always present over the liquid in the flask. The aim of this gas reservoir was to simulate to some extent a continuous capture of $CO_{2(g)}$, with different initial $[CO_{2(aq)}]$ concentrations in the aqueous medium. Because the total aqueous reaction volume was constant, the diffusion distance of $CO_{2(g)}$ was the same in all experiments.

The $CO_{2(aq)}$ concentration in the volume X of water after bubbling, was determined by titration with 0.1 M NaOH, using phenolphtaleine as the end point coloration indicator. A small quantity (~1 mg) of CA enzyme was added in the water in order to observe a sharper coloration transition, as recommended by Underwood [14]. The present titration experiments provided a $[CO_{2(aq)}]$ concentration slightly lower than the saturation value ($[CO_{2(aq)}]_{sat} \approx 39.83$ mmol L^{-1} under a $CO_{2(g)}$ gas pressure of 0.1 MPa), derived from the experimental Henry's law published by Carroll et al. [15] and Crovetto [16]. Actually, the present titration results depended on the rapidity with which the titration was performed, a result which can be explained by a progressive desorption of $CO_{2(aq)}$, when the present volume X was let in contact with the laboratory atmosphere to perform the titration (total time of ~10 min). Consequently, an initial $[CO_{2(aq)}]$ concentration of 39.83 mmol L^{-1}, in agreement with the published Henry's law [15,16] under a P_{CO_2} gas pressure of 0.1 MPa, was retained. In all the data reported in this study, the initial $CO_{2(aq)}$ content was simultaneously presented, first as the experiment volume X (mL) of initially $CO_{2(aq)}$ saturated water used, secondly as the initial molar concentration of $[CO_{2(aq)}]_0$, in the liquid reaction medium (27 mL), calculated from this saturation concentration.

A first set of experiments were carried out at ≈20 °C and the mass of solid $CaCO_{3(s)}$ formed was determined as a function of the buffer characteristics. Table 1 shows that, contrary to the buffer stock solutions used, the buffer capacity achieved in the reaction medium after 1 min reaction increased when the initial stock buffer pH increased. This result is a simple consequence of the H^+ ions formed in the water after saturation with $CO_{2(g)}$ (equilibrium pH ≈ 5.7 before buffer and $CaCl_2$ addition). These H^+ cations decreased the overall reaction medium pH, by comparison with the stock buffer solutions. Consequently, 1 min after reaction, the reaction pH was closer to the buffer pK_a when the stock solution at initial pH 10.5 was used and, farther from this pK_a with the buffer stock solution at initial pH 8.4. The initial overall ionic strength in the reaction medium was essentially due to the dissolved $CaCl_2$, and hence it had a roughly similar initial value $I \approx 0.082$ in all experiments.

The formation kinetics of $CaCO_{3(s)}$ as a function of the time were measured after addition of $T = 5$ mL buffer, in $X = 20$ mL CO_2 saturated water. For this purpose, a series of 4 similar tests were carried out and the precipitate was filtered after respectively 1, 5, 10 or 15 min reaction. A limited number of repeated tests showed that the solid mass was known with an incertitude of ~5% after 1 min, while for longer reaction times the incertitude was better: ~2% after 5 min and ~1% at longer times. The pH of the filtered solution was also measured. In further experiments, the pH 10.5 buffer was selected.

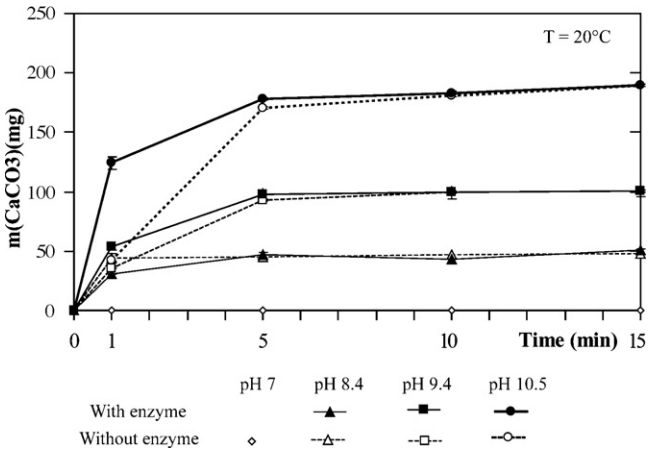

Fig. 1. Kinetics of $CaCO_3$ formation with $X = 20$ mL CO_2 saturated water, buffer volume $T = 5$ mL and $Y = 2$ mL, for buffer stock solutions at pH of 7, 8.4, 9.4 and 10.5, at 20 °C.

In a second set of experiments, the influence of the enzyme content (from 0 to 10 U, total) on the initial precipitation rate of the solid, was studied for a volume $X = 20$ mL of CO_2 saturated water and $T = 5$ mL of buffer at initial pH 10.5, at 20 °C. The mass of $CaCO_3$ formed after 1 min provided an "apparent" initial formation rate, termed V_0 (mg min^{-1}) without enzyme or $V_{0,E}$ with the enzyme, in the present study

In a third set of experiments, the initial formation rate of $CaCO_{3(s)}$ was measured for several values of X (1, 2, 5, 10 and 20 mL) and T (1, 5 and 10 mL). As previously mentioned, the total volume was always $X+T+Y = 27$ mL, a pH 10.5 buffer was used and the temperature was either ≈20 or ≈5 °C. The initial precipitation rate, during the first minute and pH achieved after this minute, were also measured. The final mass of $CaCO_{3(s)}$ formed was determined after 1 h reaction, in most case without enzyme, because all experiments showed no significant difference between the mass of solid carbonate formed with or without enzyme, beyond 15 min reaction.

3. Results and discussion

3.1. Influence of the buffer characteristics

The formation kinetics of $CaCO_{3(s)}$ after addition of $T = 5$ mL buffer at different initial pHs, for a constant volume of $CO_{2(aq)}$ saturated water $X = 20$ mL, are reported in Fig. 1. The pH change with time are reported in Fig. 2. According to Fig. 1, the mass of $CaCO_{3(s)}$ precipitated increased very quickly with time during the first minute. This first period can be explained by a formation of

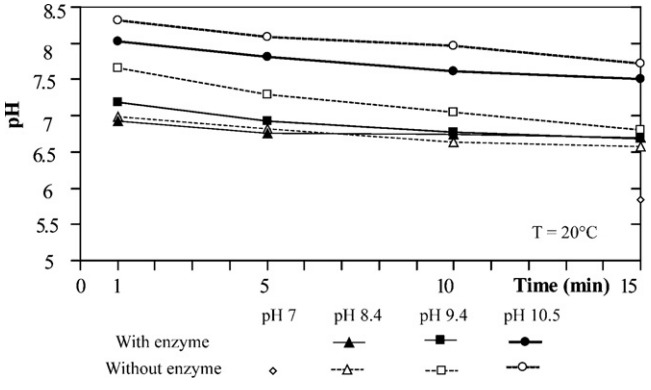

Fig. 2. Change of the pH with time, in the filtered liquid, with $X = 20$ mL CO_2 saturated water buffer volume $T = 5$ mL and $Y = 2$ mL, for buffer pH of 7, 8.4, 9.4 and 10.5, at 20 °C.

HCO_3^- anions catalysed by the enzyme. These anions were immediately converted to CO_3^{2-} by the buffer. On the other hand, the pH was too low beyond 5 min reaction. Hence, after this time, the rate limiting step in the precipitation process was the neutralization by the buffer of the H^+ formed as of reaction (3). These kinetics beyond 5 min did not depend on the presence or not of the enzyme, but only on the buffer strength and capacity.

Fig. 3 shows that the mass of precipitated $CaCO_{3(s)}$ after 15 min reactions, only depended on the buffer stock solution pH. As illustrated in Fig. 4, the apparent initial precipitation rate V_0 remained roughly constant without any enzyme for a stock solution buffer pH ≥ 8.4, while it kept increasing significantly with this buffer pH when adding the enzyme.

Moreover, for the stock buffer at pH 8.4, the initial precipitation rate without any enzyme V_0, was faster than with the enzyme ($V_{0,E}$). This apparently surprising result, as well as the kinetics results reported in Figs. 1 and 4, can actually be explained by the transformation of CO_2, traditionally described by a succession of equilibrium reactions as in scheme (2):

$$\underset{\text{step1}}{CO_{2(g)} \rightleftharpoons CO_{2(aq)} + H_2O} \underset{k_{-h}\ (\text{or } k_{-hE})}{\overset{k_h\ (\text{or } k_{hE})}{\rightleftharpoons}} \underset{\text{step 2}}{HCO_3^- + H^+} \underset{\text{step 3}}{\rightleftharpoons CO_3^{2-} + 2H^+} \quad (2)$$

In this scheme, k_h and k_{hE} designate rate constants, respectively without and with an enzyme and $CO_{2(aq)}$ designates all molecular CO_2 species in solution [12,13,17]. After bubbling $CO_{2(g)}$ in deionized water, in step 1 below, the final pH was ≈5.7 for all experiments, so that the initial CO_3^{2-} and HCO_3^- anions were in negligible concentration [18].

When a base B and/or some CA enzyme, plus some Ca^{2+} cations were added in the solution, the chemical equilibrium was displaced as indicated in scheme (3), due to the precipitation of solid $CaCO_{3(s)}$ [7,13]:

$$\underset{\text{step 1}}{CO_{2(g)} \rightarrow CO_{2(aq)} + H_2O + 2B} + \underset{\text{step 2}}{Ca^{2+} \overset{k_{hB}\ (\text{or } k_{hE})}{\rightarrow} HCO_3^- + BH^+ + B} + \underset{\text{step 3}}{Ca^{2+} \rightarrow \underline{Ca^{2+}CO_3^{2-}}_{s}\downarrow + 2BH^+} \quad (3)$$

In this scheme, k_{hB} designates a rate constant when a base such as RNH_2 is added. For simplicity, the Cl^- anions from $CaCl_2{\cdot}2H_2O$ are not shown. Nevertheless, these Cl^- anions altogether with the Ca^{2+} cations were the major contributors to the total initial ionic strength of the reaction medium, which was roughly similar in all experiments. The Cl^- anions also formed HCl molecules by capturing H^+ ions in competition with the base RNH_2 as the reactions in scheme (3) proceeded.

The reaction scheme (2) shows that the overall transformation rate of $CO_{2(aq)}$ to $CaCO_{3(s)}$, successively involves: first the formation of HCO_3^- (step 2 in the scheme (2)) and secondly the precipitation of $CaCO_{3(s)}$ (step 3). However, only step 2 (formation of HCO_3^-) can be catalyzed by the enzyme step 2. When a buffer solution at pH 8.4 was initially added in the reaction medium, Table 1 shows that, after 1 min, the pH in this reaction mixture was close to 7. This is a pH value where the CA enzyme usually operates in human bodies and is very active [9]. Hence, step 2 (formation of HCO_3^-) was certainly faster with the enzyme than without it ($k_{hE} > k_{hB}$ [7,17,19]). Because H^+ cations are formed altogether with HCO_3^- during this step, the pH also decreased to lower values with the enzyme, than without it. Besides, this reaction pH was relatively far below the RNH_2 buffer pK_a (≈8.1), in a domain where this buffer capacity β was indeed low (Table 1) and decreased very steeply as the pH decreased. In turn, step 3 (formation of CO_3^{2-} and $CaCO_3$ precipitation) was consequently slower with the enzyme than without it. Overall, the combination of steps 2 and 3 was such that, although the enzyme was faster in step 2, the overall formation rate of $CaCO_{3(s)}$ was slower with the enzyme than without it.

When the stock buffer solution at pH 10.5 was used, the enzyme remained faster to accomplish step 2. However, in this case, the initial reaction pH was close to the RNH_2 buffer pK_a, in a pH domain where the buffer capacity β was high and did not change drastically with the pH. Hence the rate of step 3 was relatively similar with or without enzyme. Overall, the formation rate of $CaCO_{3(s)}$ was therefore faster with the enzyme, than without it.

With the stock buffer solution at pH 9.4, the situation was intermediate between the two previous ones. Overall the total $CaCO_{3(s)}$ precipitation rate (during the 1st min) was still faster with the enzyme than without it, although the difference in magnitude was lower than with the buffer at initial pH 10.5.

The final mass of solid $CaCO_{3(s)}$ formed after 15 min reaction (Figs. 1 and 3) followed the same trend as the initial precipitation rate. It increased with the pH of buffer stock solution. At pH 7, the solubility limit of $CaCO_{3(s)}$ is very low and it depends on the crystallographic form, but it also increases as the pH decreases at a constant temperature [20]. Hence, for a constant volume $T = 5$ mL of the buffer solutions presently used, precipitation occurred in a lower pH range as the pH of the buffer stock solution used decreased. In turn, this precipitation stopped when the soluble $CaCO_3$ was in higher concentration as this pH decreased (Fig. 2).

3.2. Influence of the enzyme concentration

As discussed in Section 3.1, an excessive acceleration of step 2 (formation of HCO_3^-), may kill the rate of step 3 (formation of CO_3^{2-}). A similar effect was observed when the mass of enzyme was increased. Overall, Fig. 5 shows that the enzyme drastically increased the magnitude of the initial "apparent" precipitation rate of $CaCO_{3(s)}$, determined after 1 min reaction, by comparison with a reaction without enzyme. This apparent initial rate increased by a factor >10 when 4 mg CA enzyme were added in the reaction at 5 °C. However, Fig. 5 also shows that increasing the mass of enzyme did

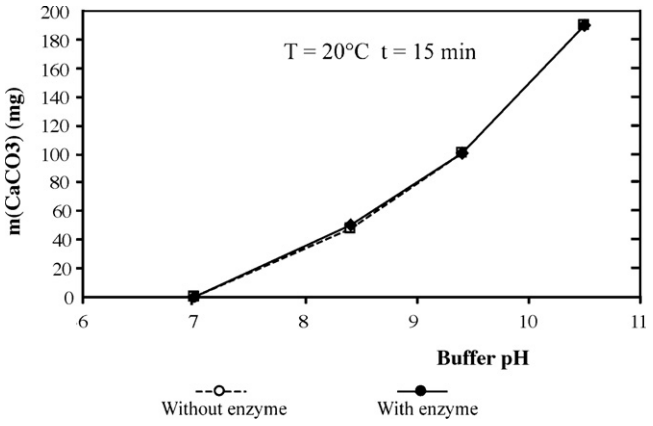

Fig. 3. Mass of $CaCO_{3(s)}$ formed 15 min after 5 mL buffer addition ($Y = 2$ mL), as a function of the initial buffer pH, at 20 °C.

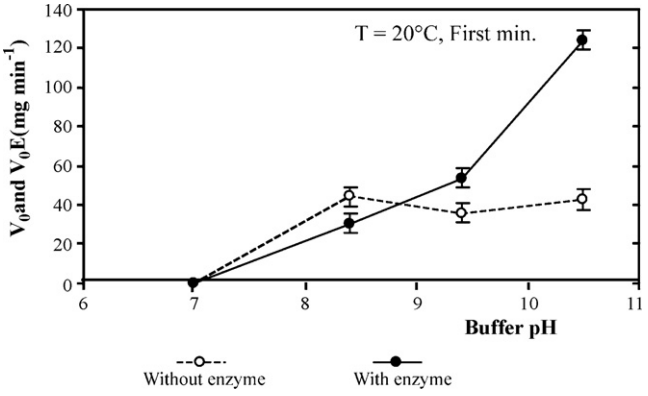

Fig. 4. Initial formation rate of $CaCO_{3(s)}$ (during the 1st min) after 5 mL buffer addition (Y = 2 mL), as a function of the stock solution buffer pH at 20 °C.

not necessarily increase the total initial formation rate of $CaCO_{3(s)}$. An optimum quantity of enzyme exists, for which the initial precipitation rate of $CaCO_{3(s)}$ was maximum. In the present study, the optimum quantity of enzyme was ≤1 mg (1.3 U). This apparently surprising result can indeed be explained by the same mechanism as discussed just before, for the buffer stock solution at pH 8.4. Beyond the maximum, increasing the mass of enzyme accelerates step 2 (formation of HCO_3^- and H^+) in reaction (3) to a faster rate. Hence the pH also decreases at a faster rate towards lower values. In turn, this decelerates step 3 (precipitation of $CaCO_{3(s)}$). Overall, the initial precipitation rate of $CaCO_{3(s)}$, $V_{0,E}$, may therefore decrease, in agreement with Fig. 5.

At the end, the total mass of $CaCO_{3(s)}$ precipitated did not depend on the presence of the enzyme which, as a catalyst, can only change the kinetics to reach equilibrium, not the equilibrium thermodynamics. Our results were in agreement with these expectations since the mass of solid formed after a long time (15 min) was similar with or without CA enzyme, for a given buffer stock solution (Fig. 1).

3.3. Influence of the volume X of saturated CO_2 water and the volume T of pH 10.5 buffer

The initial formation rate of $CaCO_{3(s)}$ for several values of CO_2 saturated water volume X (1, 2, 5, 10 and 20 mL) and pH 10.5 buffer volume T (1, 5 and 10 mL), at a constant total reaction liquid volume $X+T+Y$ = 27 mL, are reported in Figs. 6 and 7, for a reaction temperature of 20 °C and at 5 °C, respectively. This initial formation rate was an apparent rate, determined from the mass of $CaCO_{3(s)}$ precipitated after 1 min reaction. Indeed, some solid $CaCO_{3(s)}$ was precipitated with or without the enzyme but a stock buffer volume $T \geq 5$ mL was necessary to observe a significant difference between the initial formation rates $V_{0,E}$ and V_0, respectively with and without enzyme. This can again be explained by the buffer capacity in the reaction medium. A higher stock buffer volume T made it possible to increase the initial pH in the reaction medium, hence the buffer capacity in this reaction medium, so that the kinetics rate of step 3 (formation of $CaCO_{3(s)}$) in scheme (3) increased.

Besides, for T = 5 and 10 mL, the initial formation rate of $CaCO_{3(s)}$ also increased linearly with X, for X > 2 mL. The linear increase coefficient was independent of the value of T and the presence or absence of CA enzyme. This linear regime may therefore be due to another type of rate limiting step, such as for instance an added dissolution of $CO_{2(g)}$ to $CO_{2(aq)}$ according to reaction (2) by diffusion from the atmosphere above the water into the reaction media.

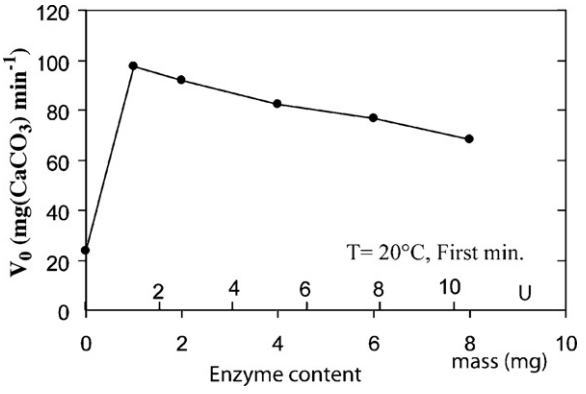

Fig. 5. Initial formation rate $V_{0,E}$ of $CaCO_{3(s)}$ as a function of the quantity of CA enzyme for a volume X = 20 mL of CO_2 saturated water solution, a volume T = 5 mL of the buffer stock solution at pH 10.5, a total water volume of 27 mL and 0.3 g of $CaCl_2{\cdot}2H_2O$, at 20 °C.

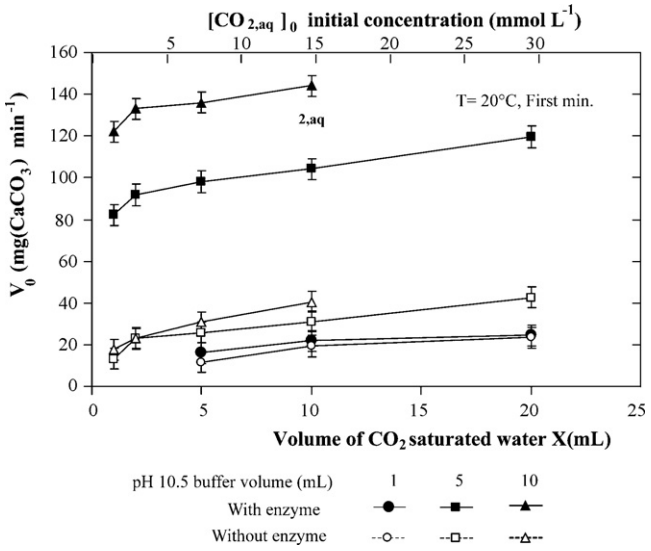

Fig. 6. Initial formation rate V_0 and $V_{0,E}$ of $CaCO_{3(s)}$ as a function of volume X of saturated water and a volume T = 5 mL of the buffer stock solution at pH 10.5, for a total water volume of 27 mL and 0.3 g $CaCl_2{\cdot}2H_2O$, at 20 °C.

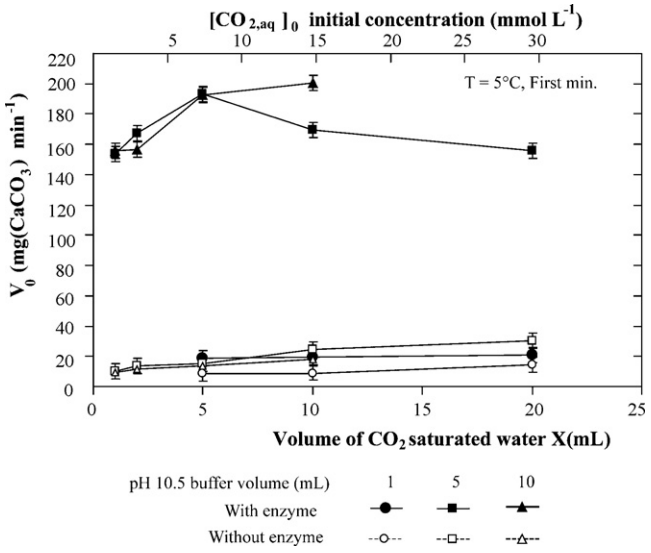

Fig. 7. Initial formation rate V_0 and $V_{0,E}$ of $CaCO_{3(s)}$ as a function of volume X of saturated water and a volume T = 5 mL of the buffer stock solution at pH 10.5, for a total water volume of 27 mL and 0.3 g $CaCl_2{\cdot}2H_2O$, at 5 °C.

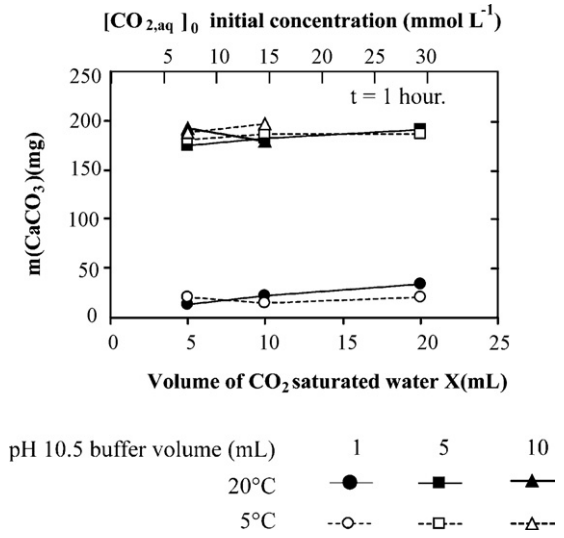

Fig. 8. Mass of $CaCO_{3(s)}$ formed after 1 h, without enzyme, as a function of the saturated water volume X and volume T of the buffer stock solution at pH 10.5, at 20 °C (solid marks) and 5 °C (white marks).

Interestingly, the initial rate data obtained in an iced bath showed no significant difference between the stock buffer volumes T = 5 and 10 mL (Fig. 7). The most outstanding result was that the mass of solid $CaCO_{3(s)}$ formed passed through a reproducible maximum when the volume of CO_2 saturated water was X = 5 mL, only for T = 5 mL. This suggests that a transformation of the solid first formed, occurred during ageing in the aqueous medium, a phenomenon which is discussed in a further section of this text.

By comparison with the initial rate data, the mass of $CaCO_{3(s)}$ precipitated after 1 h reaction was similar for the stock buffer volumes T = 5 and 10 mL (Fig. 8), both at 5 and at 20 °C. This final mass was also very close from the mass expected for a total conversion of the added $CaCl_2{\cdot}2H_2O$ to $CaCO_{3(s)}$ (204 mg). Such a nearly constant precipitate mass was consistent with the presence of an excess of CO_2 available, comprising the $CO_{2(aq)}$ in the initial volume X of water, plus the $CO_{2(g)}$ from the gas atmosphere above the water.

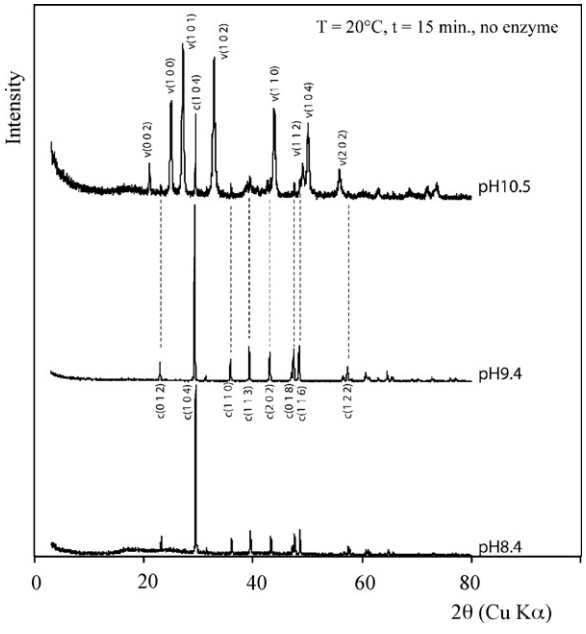

Fig. 9. X-ray diffraction spectra of the solid $CaCO_{3(s)}$ made with X = 20 mL saturated water and T = 5 mL of buffer stock solutions at different pHs, without enzyme, after 15 min reaction at ≈20 °C (Cu Kα radiation).

Indeed, as previously mentioned, the flask containing the $CO_{2(aq)}$ saturated water volume X was maintained closed with rubber septum, after the saturation operation under a $CO_{2(g)}$ pressure 0.1 MPa. Hence, as soon as some $CaCO_{3(s)}$ begun to precipitate, some more $CO_{2(g)}$ diffused from the flask gas phase into the aqueous medium, as indicated by the arrow corresponding to step 1 in scheme (3). On the other hand, when only T = 1 mL stock buffer was added, the limiting step in solid precipitation was the low pH reached in the reaction medium (Fig. 8), in relationship with a low buffer capacity at low pH.

Overall, the global formation rate of $CaCO_{3(s)}$ in the present "one pot" process, cannot be approximated by a simple equation such as the Michaelis law. The main reason is that the present global precipitation process combined several contributions. A first contribution was the transformation of the $CO_{2(aq)}$ initially dissolved in the volume X of water. A second one was due to the replacement of the $CO_{2(aq)}$ initially transformed, with new $CO_{2(aq)}$, coming by diffusion from the gas phase. A third more complex contribution was the formation of two different solid phases, vaterite and calcite, with different solubility limits [20].

3.4. Characterization of the solid carbonate formed

Without any enzyme, the crystallographic structure of $CaCO_{3(s)}$ formed after 15 min reaction depended on the stock buffer pH used

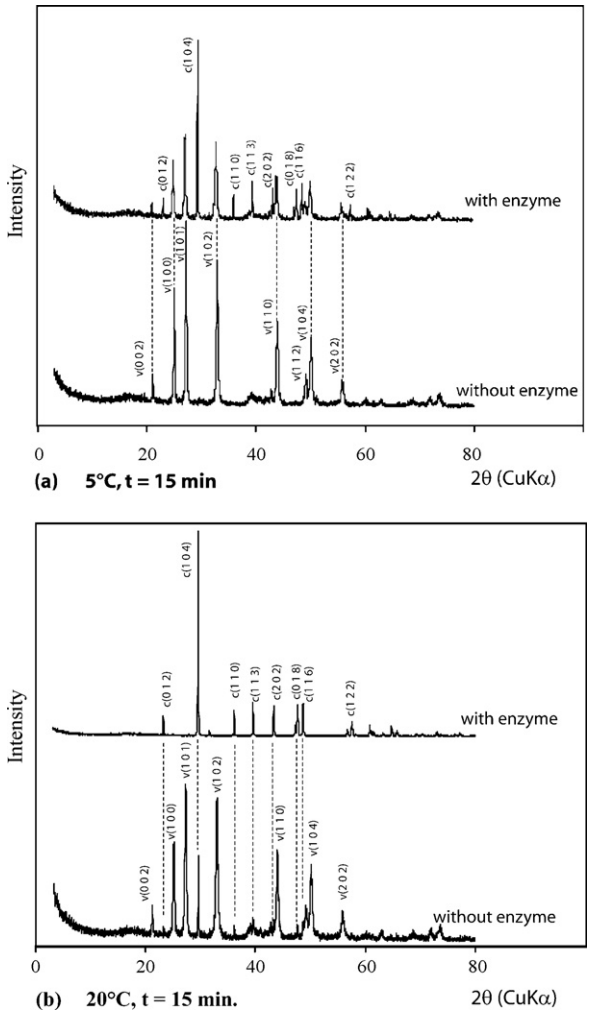

Fig. 10. X-ray diffraction spectra of the solid $CaCO_3$, made with X = 20 mL saturated water and T = 5 mL of buffer stock solution at pH 10.5, with or without enzyme, after 15 min reaction: (a) at ≈5 °C and (b) at 20 °C (Cu Kα radiation).

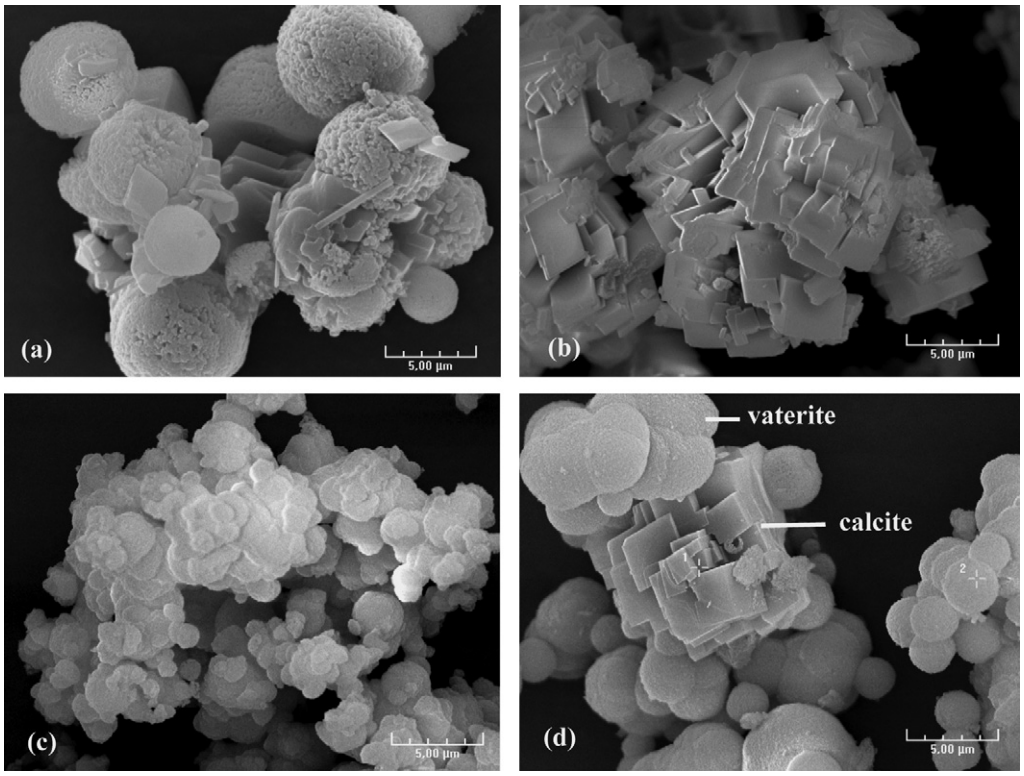

Fig. 11. Scanning electron micrographs (SEM) of the solid $CaCO_{3(s)}$ made with X = 20 mL saturated water and T = 5 mL of buffer stock solution at pH 10.5, after 15 min reaction: (a) at ≈5 °C with enzyme; (b) at 20 °C with enzyme; (c) at 5 °C without enzyme; (d) at 20 °C without enzyme.

(Fig. 9). In particular, at 20 °C with X = 20 mL of CO_2 saturated water and T = 5 mL stock buffer at pH 8.4 or 9.4, the X-ray diffraction spectra only showed the thermodynamically stable calcite phase, while the metastable vaterire phase dominated when the stock buffer at pH 10.5 was used (Fig. 9). On the other hand, still with the latter pH 10.5 stock buffer, adding some CA enzyme favoured the conversion of vaterite to calcite, both at 5 and 20 °C (Fig. 10). The temperature also had some influence, since at 20 °C this conversion was complete, while at 5 °C this conversion was partial.

Changes in the crystallographic structure and/or shape of solid particles with time, are commonly observed when solid particles are grown in a liquid medium [21]. In particular, such phenomena were reported regarding solid carbonate particles, in some case precipitated with the help of a urease enzyme [22–25]. Three different types of mechanisms are known to explain such solid transformations. A first one is a change in the growth mechanism, from the so-called mononuclear mode to either the polynuclear or the diffusion controlled mode. No crystallographic change in the nature of the particles is observed in this case. A second type of mechanism is known to occur during aging and involves the dissolution of a first burst of particles, followed by re-precipitation to a new more stable crystallographic phase. In this case, the crystallographic nature of the solid changes with time. A third possible mechanism could be combined with the previous aging mechanism, because it is known that the side amino groups of proteins may influence the nature of the hydrolysis products from the solid precursor [25,26]. However the enzyme content in the present tests was very low, so that this mechanism was unlikely. Overall, because a phase change from vaterite to calcite was presently observed, we consider that the mechanism which operated was the second one: dissolution-reprecipitation during aging. In this case, the effect of the carbonic anhydrase was only to accelerate the formation of HCO_3^- followed by CO_3^{2-} anions. Hence it permitted the whole aging process to begin more rapidly, which ended in a faster formation of the stable calcite phase. On the other hand, the FTIR transmission spectra did not show the presence of $Ca(OH)_2$ in any solid formed with the 4 stock buffer solutions used in this study.

The scanning electron micrographs characteristics of the vaterite and calcite particles obtained are illustrated in Fig. 11. Both $CaCO_3$ varieties adopt a hexagonal structure [27,28], but vaterite is more complex with a packing which leads to the growth of spherical particles. On the other hand, the calcite crystals displayed well defined faceted rhombohedral characteristics. Their formation by a dissolution reprecipitation of the vaterite particles is supported by Fig. 11a (with enzyme at 5 °C), which showed the spherical vaterite particles were very porous, while the thin planar calcite crystals were not porous and they had grown on the external surface from the vaterite particles.

4. Conclusions

The present paper showed that the carbonic anhydrase enzyme accelerated the formation rate of solid carbonate from $CaCl_2{\cdot}2H_2O$ and CO_2 by a factor >10 at 5 °C, when a buffer stock solution at pH 10.5 was used. The initial precipitation rate of the solid depended on the capacity and strength of the initial buffer stock solution used and on the quantity of enzyme. An acceleration of the formation rate of HCO_3^- anions, either with the buffer or an increasing mass of enzyme, may decrease the pH at a rate so fast that the overall precipitation of $CaCO_{3(s)}$ rate may itself decrease. Depending on the conditions, the formation of two different $CaCO_3$ phases was observed: vaterite and calcite. The first one was precipitated at pH 10.5, when the enzyme was absent. It was the only phase observed at 5 °C, pH 10.5, without any enzyme. A lower pH, or at 20 °C when the enzyme was added, the formation of calcite was favoured.

References

[1] S.M. Benson, T. Surles, Proc. IEEE 94 (10) (2006) 1795–1805.
[2] H. Matsuyama, A. Terada, T. Nakagawara, Y. Kitamura, M. Teramoto, J. Membr. Sci. 163 (1999) 221–227.
[3] J. Ge, R.M. Cowan, C. Tu, M.L. McGregor, M.C. Trachtenberg, Life Support Biosphys. Sci. 8 (2002) 181–189.
[4] G.P. Knowles, J.V. Graham, S.W. Delaney, A.L. Chaffee, Fuel Process. Technol. 86 (2005) 1435–1448.
[5] M.M. Maroto-Valera, D.J. Fauthb, M.E. Kuchtaa, Y. Zhanga, J.M. Andreïsena, Fuel Process. Technol. 86 (2005) 1627–1645.
[6] T. Sakakura, J.-C. Choi, H. Yasuda, Chem. Rev. 107 (2007) 2365–2387.
[7] M.L. Druckenmiller, M. Mercedes Maroto-Valer, Fuel Process. Technol. 86 (2005) 1599–1614.
[8] S. Lindskog, Pharmacol. Ther. 74 (1997) 1–20.
[9] L. Bao, M.C. Trachtenberg, J. Membr. Sci. 280 (2006) 330–334.
[10] N. Liu, G.M. Bond, A. Abel, B.J. McPherson, J. Stringer, Fuel Process. Technol. 86 (2005) 1615–1625.
[11] G.M. Bond, J. Stringer, D.K. Brandvold, F.A. Simsek, M.-G. Medina, G. Egeland, Energy Fuels 15 (2001) 309–316.
[12] Y. Pocker, D.W. Bjorkquist, J. Am. Chem. Soc. 99 (1977) 6537–6543.
[13] P. Mirjafari, K. Asghari, N. Mahinpey, Ind. Eng. Chem. Res. 46 (2007) 921–926.
[14] A.L. Underwood, Anal. Chem. 33 (1961) 955–956.
[15] J.J. Carroll, J.D. Slupsky, A.E. Mather, J. Phys. Chem. Ref. Data 20 (1991) 1201–1209.
[16] R. Crovetto, J. Phys. Chem. Ref. Data 20 (1991) 575–589.
[17] P.V. Danckwerts, Chem. Eng. Sci. 36 (1981) 1741–1742.
[18] L.W. Diamond, N.N. Akinfiev, Fluid Phase Equilibr. 208 (2003) 265–290.
[19] S. Lindskog, J.E. Coleman, Proc. Natl. Acad. Sci. U.S.A. 70 (1973) 2505–2508.
[20] J.-Y. Gal, J.-C. Bollinger, H. Tolosa, N. Gache, Talanta 43 (1996) 1497–1509.
[21] A.C. Pierre, Introduction to Sol–Gel Processing, Kluwer Academic Publishers, Boston, USA, 1998 (Chapter 3 Colloidal particles and Sols, pp. 91–163).
[22] L. Wang, I. Sondi, E. Matijevicˇ, J. Colloids Interface Sci. 218 (1999) 545–553.
[23] I. Sondi, E. Matijevicˇ, J. Colloids Interface Sci. 238 (2001) 208–214.
[24] K.L. Bachmeier, A.M. Williams, J.R. Warmington, S.S. Bang, J. Biotechnol. 93 (2002) 171–181.
[25] I. Sondi, E. Matijevic, Chem. Mater. 15 (2003) 1322–1326.
[26] A.C. Pierre, P. Buisson, J. Sol–Gel Sci. Technol. 38 (2006) 63–72.
[27] S.R. Kamhi, Acta Cristallogr. 16 (1963) 770–772.
[28] D.L. Graf, Am. Miner. 46 (1961) 1283–1316.